Biol Cybern (2006) 94: 97–109
DOI 10.1007/s00422-005-0018-8

ORIGINAL PAPER

Biological Cybernetics

A. A. Frolov · R. A. Prokopenko · M. Dufossè
F. B. Ouezdou

Adjustment of the human arm viscoelastic properties to the direction of reaching

Received: 15 August 2005 / Accepted: 12 September 2005 / Published online: 13 December 2005

Abstract The viscoelastic properties of the human arm were measured by means of short force perturbations during fast reaching movements in two orthogonal directions. A linear spring model with time delay described the neuromuscular system of the human arm. The obtained viscoelastic parameters ensured movement stability in spite of the time delay of 50 ms. The stiffness and viscosity ellipses appeared to be predominantly orthogonal to the movement direction, which reduced the effect of force perturbation in the direction orthogonal to the reaching movement. Thus, it can be argued that the viscoelastic properties of the neuromuscular system of the human arm are adjusted to the direction of movement according to a "path preserving" strategy, which minimizes the deviation of the movement path from a straight line, when exposed to an unexpected external force.

1 Introduction

The human arm is supplied by two mechanisms of feedback control which stabilize arm movements provoked by the central motor commands. The first concerns the mechanical properties of muscles. In the case of constant activation, muscle force depends on both muscle length and muscle velocity. The second mechanism concerns the regulation of muscle activity by stretch reflex loop, which also depends on muscle length and muscle velocity. An important property of the stretch-reflex feedback is its time delay of the order of tens of milliseconds. Both mechanisms provide position and velocity feedback influencing joint torques. The feedback gains are called stiffness and viscosity, respectively.

Many experiments showed that these viscoelastic properties of the neuromuscular system are task dependent. Particularly joint stiffness during posture maintenance (Tsuji et al. 1995) differs from that during reaching movement (Gomi and Kawato 1997). Joint stiffness depends on the direction of external loading during posture maintenance (Gomi and Osu 1998) as well as on the direction of reaching movement (Gomi and Kawato 1997; Mah 2001), and it can be adjusted to the task (Lacquaniti et al. 1993; Biryukova et al. 1999). A change in joint stiffness can be explained by the co-activation of antagonist muscles and by the nonlinear force-length dependence of each individual muscle. An approximately exponential dependence of muscle force on muscle length (Feldman 1979) results in a linear dependence of muscle stiffness on muscle force (Shadmehr and Arbib 1992). Thus, activation of an individual muscle always produces proportional increases in both the joint torque and the joint stiffness. By contrast, co-activation of antagonist muscles results in an increase of the joint stiffness independently of the total joint torque.

In the experiments of Lacquaniti et al. (1993) and Biryukova et al. (1999), the anticipatory increase of stiffness can be explained by co-activation of antagonistic muscles without any change in the total joint torque. The functional meaning of this co-activation is to prevent any future external perturbation due to fast loading or unloading of the arm. In the experiments of Gomi and Osu (1998), the change of stiffness can be explained by an activation of the muscles resisting the external force, and with almost no activation of antagonistic muscles. In this case the increase in stiffness was roughly proportional to the increase in joint torque. The functional meaning of the change in joint stiffness depending on the direction of reaching, as observed by Gomi and Kawato (1997) and Mah (2001), is not clear. The main goal of the present paper is to analyze the functional meaning of these changes in stiffness. Our hypothesis is that the viscoelastic

A.A. Frolov · R.A. Prokopenko (✉)
Institute of Higher Nervous Activities and Neurophysiology,
Russian Academy of Sciences, Moscow, Russia
E-mail: rprok@mail.ru
Tel.: +7-095-3344231
Fax: +7-095-3388500

M. Dufossè
Laboratory INSERM U483, University Pierre and Marie Curie,
Paris, France

F.B. Ouezdou
Laboratory LIRIS - CNRS FRE 2508, University of Versailles
Saint-Quentin-en-Yvelines, Vélizy, France

properties are adjusted to the direction of the reaching movement in order to prevent deflections from the planned trajectory caused by unexpected external force perturbation.

We studied the reaching movements of the right hand in two orthogonal directions in a horizontal plane: to the right and forward. In order to determine the viscoelastic properties of the arm, three types of perturbations are commonly used: (1) unpredictable, systematic perturbations provoked by a force field, such as a spring of unknown stiffness (Domen et al. 1999; Cesari et al. 2001), or by external geometrical constraints, such as a "virtual wall" (Mah 2001); (2) perturbations applied stochastically during the whole movement (Bennett et al. 1992; Tsuji et al. 1995); and (3) short, transient perturbations applied during different phases of the movement (Gomi and Kawato 1997; Gomi and Osu 1998). Each of these methods presents advantages and disadvantages. The advantage of the first method is that it allows for continuous estimation of viscoelastic parameters during the whole movement. Its disadvantage concerns the problem of central correction of the systematic perturbation. Although subjects are usually asked to perform a standard movement and "not to intervene" if external conditions change, the central correction cannot be completely excluded, because it is much more natural for humans to respond to systematic perturbation than not to respond. The second method overcomes this disadvantage. However, a stochastic perturbation can result in joint stiffening due to muscle co-contraction and thus in changes of the viscoelastic parameters from normal values (Bennett 1994; Stein and Kearney 1995). Although the third method, i.e. the short random perturbations of Gomi and Kawato (1997), requires many experimental trials, we decided to use it in our experiments because it avoids the possible systematic errors mentioned above.

Although the neuromuscular system is nonlinear, most research uses linear, spring-like models as a first approximation of its viscoelastic properties. In these models, elastic and viscous components of the joint muscle torques are assumed to be linearly dependent on joint angles and angular velocities. The general inadequacy of this approach was emphasized by Winters and Stark (1987): linear models operate with lumped system parameters (stiffness and viscosity), which are only indirectly related to the well-known, main mechanisms of muscle force generation, i.e., alpha-motoneuron recruitment, intrafusal transduction, muscle fiber activation due to calcium kinetics, actin–myosin interaction and so on. For these reasons, linear models cannot be applied to investigate the whole range of the muscle force generation. In their view, describing arm properties by lumped parameters such as stiffness and viscosity is no more than "playing with interpolation". The papers of Flanagan et al. (1993) and Gribble et al. (1998) agree with this criticism. However, Frolov (2000) showed that, for reaching movement, a linear spring-like model that includes a time delay will accurately approximate the nonlinear model used by Gribble et al. (1998) That is why in this study we have used such a model to describe the viscoelastic properties of the neuromuscular system of the arm.

2 Method

Four voluntary, right-handed male subjects, aged 21–51 years participated in the study. They had no known history of a motor disorder. All the subjects provided informed consent prior to testing.

2.1 Experimental set-up

The subject sat with his trunk attached by a belt to the rigid back of the chair. The subject produced reaching movements with his right hand in the horizontal plane at shoulder level. Two vertical ropes hanging from the ceiling were tied round the fore- and upper arm to counteract gravity. A molded plastic cuff (mass 0.245 kg) restricted wrist movement and kept the forearm in a pronated position. Thus, the hand and the forearm moved as a single segment, and hence the arm had only two degrees of freedom: flexion-extension in the shoulder joint and flexion-extension in the elbow joint.

Movement perturbations were produced by means of three strings (Fig. 1) attached to the plastic cuff below the center of the palm. After one of the strings, randomly chosen, was pulled, it passed via a system of pulleys to a small electromagnet (*M2*) attached to a load (weight about 6 kg). At the beginning of each trial, the load was held by another large electromagnet (*M1*) placed about one meter above the floor. Unlike the small electromagnet, the large one was fixed to the wall so that the force initially applied to the hand was zero. When the computer switched off this large electromagnet, the load fell and tightened the string. Then a spring (*S*) pulled back the load, and the tension of the string dropped to zero. At this moment the small electromagnet was switched off and the string became disconnected from the load. Tension of the string perturbed the arm in a direction determined by one of the three pulleys. One pulley was located in front of the subject and the two others at about 60° to the right and to the left. The force produced by the string was measured by a strain gauge, whose static accuracy was 0.1 N.

Arm motion was recorded with a MiniBird^{TM} system, which used an electromagnetic field to determine the 3D position and orientation of its sensors in relation to a stationary base. Three sensors operating at a rate of 100 Hz were used. The static accuracy of the MiniBird^{TM} was 0.18 cm for sensor positions and 0.5° for sensor orientations. Hand acceleration was recorded with a 3D accelerometer ADXL150 of Analog Devices. The accelerometer signals were sampled at 1 kHz with accuracy of 0.06 m/s^2 . The accelerometer and one MiniBird^{TM} sensor were fixed to a plate that was attached with adhesive tape to the dorsal surface of the hand. The coordinate systems of the accelerometer and the MiniBird^{TM} sensor were matched. Since acceleration is measured in the coordinate system of the accelerometer, the sensor orientation was required to obtain hand acceleration relative to the stationary base. The two other MiniBird^{TM} sensors were placed on the dorsal surface of the upper arm (at approximately 15 cm above the trochlea humeri) and at the highest

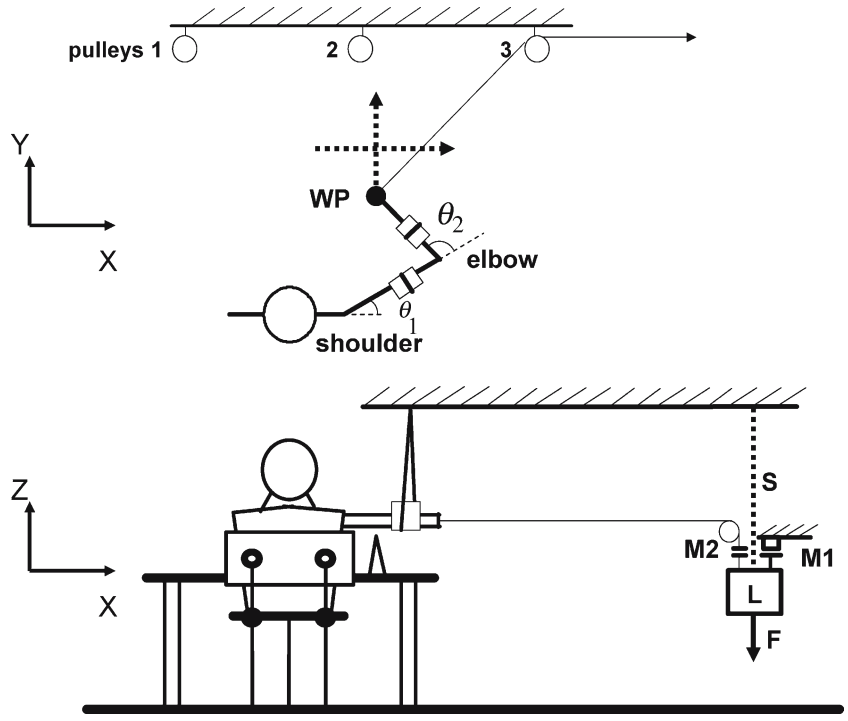

Fig. 1 Experimental setup

point of the acromion. The center of the palm was considered as a working point (WP) during reaching.

2.2 Procedures

Three series of recordings were performed for each subject.

The first series was aimed at localizing the anatomical axes of flexion-extension in the shoulder and elbow joints. In this series, the subject was asked to relax and to allow the experimenter to execute sequences of 5–8 rotations around each of these two axes. The rotation amplitudes were 0.7–0.8 of maximal physiological range.

The second series was aimed at determining the inertial parameters of the arm. The subject was asked to keep WP above the tip of a small cone fixed on a table below the plane of movements. The arm was perturbed at two different WP positions: one at 20 cm forward and the other at 30 cm forward and 15 cm to the left of the shoulder joint. For each position, four types of trials were performed, three with perturbations directed toward one of the three pulleys and one without perturbation. The latter was used to check the absence of central prediction and correction of perturbation. The subject was instructed not to intervene during the perturbation. These four types of trials were altered pseudo-randomly. Each type was executed four times in each WP position. The subject could predict neither the type, nor the moment of perturbation.

The third series was aimed at determining the viscoelastic properties of the arm during movement. The reaching movements were performed in two orthogonal directions (Fig. 1): transversal movement from 15 cm to the left to 15 cm to the right at a distance of 30 cm in front of the shoulder joint; forward movement from 20 cm to 40 cm forward of the shoulder joint. Initial and target positions were shown to the subject by two small cones below the plane of movements. Before the recording session, the subjects performed several training movements. The subjects were instructed to perform movements as fast as possible. The same four types of trials as in the second series were used. The onset of perturbation was synchronized with the onset of movement, determined by the accelerometer data.

The subjects could rest between the second and the third series and between the forward and transversal movements in the third series. The whole experiment lasted about one hour and the subjects said they did not feel fatigued.

3 Model

3.1 Dynamics

As described in previous papers (Hogan 1985; Flash 1987; Flanagan et al. 1993; Gribble et al. 1998; Shadmehr 1993; Gomi and Kawato 1997), we used a model of an arm with two links and two joints (shoulder, elbow) performing reaching movements in the horizontal plane. These movements were either unperturbed or perturbed by small horizontal external forces **F** applied to the hand. An arm movement is described by the motion equation:

$$I(\theta)\ddot{\theta} + C(\theta, \dot{\theta})\dot{\theta} = T + J^T(\theta)F \quad (1)$$

where θ is the vector of the joint angles (θ_1 for the shoulder, θ_2 for the elbow), **I** is the matrix of inertia, **C** is the matrix of centrifugal and Coriolis forces, **T** is the vector of joint muscle torques, $\mathbf{J}^T$ (transpose of Jacobian matrix **J**) transforms the small, horizontal, external force **F** applied to the hand into joint torques. Matrices **I**, **C** and **J** depend on anthropometric parameters, such as (1) the masses of the upper arm and the forearm m_1 and m_2, (2) their lengths L_1 and L_2, (3) their moments of inertia relative to the shoulder and elbow joints I_1 and I_2, and (4) the distances between their centers of mass and their corresponding proximal joints L_{c1} and L_{c2}. The coefficients of matrices **I** and **C** can be expressed by only three independent anthropometric parameters (Katayama and Kawato 1993):

$$z_1 = I_1 + I_2 + m_2 L_1^2, \quad z_2 = m_2 L_1 L_{c2}, \quad z_3 = I_2$$

and then:

$$I_{11} = z_1 + 2z_2 \cos(\theta_2), \quad I_{12} = z_3 + z_2 \cos(\theta_2)$$

$$I_{21} = I_{12}, \quad I_{22} = z_3$$

$$C_{11} = -2z_2 \sin(\theta_2)\dot{\theta}_2, \quad C_{12} = -z_2 \sin(\theta_2)\dot{\theta}_2$$

$$C_{21} = z_2 \sin(\theta_2)\dot{\theta}_1, \quad C_{22} = 0$$

The Jacobian **J** of the transformation of joint angles into hand position has the form:

$$J_{x1} = -L_1 \sin(\theta_1) - L_2 \sin(\theta_1 + \theta_2), \quad J_{x2} = -L_2 \sin(\theta_1 + \theta_2)$$

$$J_{y1} = +L_1 \cos(\theta_1) + L_2 \cos(\theta_1 + \theta_2), \quad J_{y2} = +L_2 \cos(\theta_1 + \theta_2)$$

3.2 Muscle torques

We described the dependence of joint torques $\mathbf{T}(t)$ upon joint angles $\theta(t)$ and angular velocities $\dot{\theta}(t)$ by the linear regression model with time delay τ :

$$\mathbf{T}(t) = \mathbf{T}^0(t) - \mathbf{S}(t)\theta(t-\tau) - \mathbf{V}(t)\dot{\theta}(t-\tau), \qquad (2)$$

where $\mathbf{T}^0(t)$ is intercept of the regression model, and $\mathbf{S}(t)$ and $\mathbf{V}(t)$ are the matrices of coefficients of the regression model, which can be interpreted as lumped stiffness and viscosity of the neuromuscular system. The diagonal coefficients S_{ii} and V_{ii} quantify the viscoelastic properties of shoulder ($i = 1$) and elbow ($i = 2$) muscles and their nondiagonal coefficients quantify the viscoelastic properties of biarticular muscles. The time delay τ accounts for the delay in the stretch-reflex loop and the calcium kinetics. Experimental data show that the two nondiagonal coefficients of each matrix are quite close (Tsuji et al. 1995, Gomi and Kawato 1997). In order to reduce the number of regression parameters, we put $S_{12} = S_{21}$ and $V_{12} = V_{21}$. As shown by Frolov (2000), this model with a proper choice of the time delay τ fits the complex properties of the nonlinear model of muscle force generation quite accurately. The parameters $\mathbf{T}^0(t)$, $\mathbf{S}(t)$ and $\mathbf{V}(t)$ are assumed to be centrally controlled variables, i.e., independent of short and random external perturbations.

4 Results

4.1 Arm geometry

The first series of experiments was performed in order to determine (a) the position of the elbow joint axis in relation to the hand sensor (length of the forearm), (b) the distance between this axis and the center of rotation in the shoulder (length of upper arm), and (c) the position of this center in relation to the stationary coordinate system. These data, not accessible to direct measurement, were evaluated from the kinematics recordings. The method for calculating the geometrical parameters of the arm, as described in Biryukova et al. (2000) and Prokopenko et al. (2001), provides a maximum fit of the kinematics recordings to the model representing the arm as a system of rigid bodies connected by joints with fixed geometry. The accuracy of the rigid body assumption was found to be 0.4–0.9 cm for sensor positions and 3–5° for sensor orientations in all four subjects.

4.2 Perturbation

The time course of perturbation force was smooth, without abrupt force changes at the beginning and end of the perturbation, thus avoiding fast oscillations of the accelerometer. The amplitude of perturbation was chosen from 10 to 20 N for different subjects in order to achieve the significant changes in WP position and acceleration. The time courses of perturbation forces during reaching movements in transverse and forward directions for subject#1 are shown in Fig. 2. The amplitude and shape of perturbations were rather stable. The onsets of perturbations were randomly distributed in the first half of the movement and their durations amounted to about 250 ms. Thus, the perturbation maximum fell at the second half of the movement.

4.3 Inertial parameters

In the second series, the inertial anthropometric parameters z_1, z_2 and z_3 were calculated during the earliest phase of perturbation. The earliest EMG response to abrupt perturbation has a delay of 30–60 ms (Koshland and Hasan 2000). Thus the hand acceleration in the 50 ms after the start of perturbation is mainly determined by the inertial properties of the arm. At this phase, the muscle torques **T** in motion equation (1) can be ignored. The direction of the force **F** is defined by the direction of the string, and the absolute value of the force is given by the strain gauge recordings. The angular velocity $\dot{\theta}$ was obtained from equation $\dot{\theta} = \mathbf{J}^{-1}\mathbf{v}$ where **v** is WP velocity, which was found by integrating the accelerometer data. The angular acceleration $\ddot{\theta}$ was obtained from equation $\ddot{\theta} = \mathbf{J}^{-1}(\mathbf{a} - \mathbf{a}')$, where **a** is WP acceleration, and $\mathbf{a}'$ is a vector with components $\mathbf{a}'_k = \sum_{ij} \frac{\partial J_{ki}}{\partial \theta_j}\dot{\theta}_i\dot{\theta}_j$. During the first 50 ms, when muscle torques in Eq. (1) can be ignored,

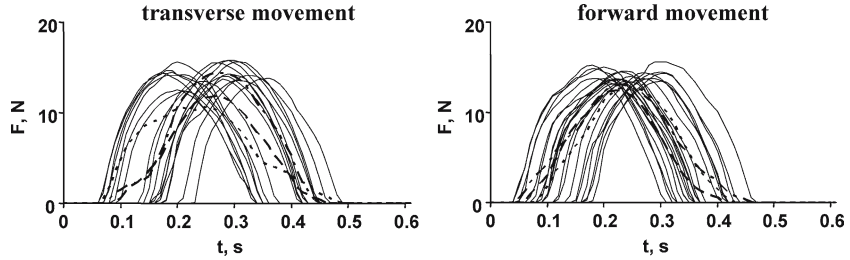

Fig. 2 Time course of perturbation force for subject#1. Zero time corresponds to the movement onset. Trajectories averaged over perturbed to the left, to the right, and forward are shown by *dashed, dotted, and dashed-dotted lines*, respectively

Table 1 Inertial anthropometric parameters (kg m^2)

Subject	z_1	z_2	z_3
1	0.386±0.017	0.155±0.013	0.090±0.003
2	0.250±0.012	0.116±0.011	0.079±0.003
3	0.230±0.010	0.079±0.009	0.063±0.002
4	0.281±0.015	0.150±0.022	0.090±0.004

this equation can be considered as a linear regression equation relative to the inertial parameters z_1, z_2 and z_3. These parameters were obtained by solving this regression equation at this initial phase of movement over the whole set of data for perturbations in different directions and for different arm positions. The results are presented in Table 1.

4.4 Reaching movements

The time courses of joint angles, angular velocities, accelerations, and muscle torques in subject#1 are shown in Fig. 3 for both movement directions and all types of trials. The muscle torques were calculated from motion equation (1). The movements were averaged across all trials in each of four types: unperturbed (solid lines), perturbed to the left (dashed lines), perturbed to the right (dotted lines), perturbed forward (dashed-dotted lines). The contribution of the shoulder joint was larger for transverse movement whereas the elbow joint was dominant for forward movement. Transverse movement was slightly longer than the forward one. For transverse movement joint angles reached final values in about 0.3 s, and for forward movement in about 0.2 s. Duration of the forward movement was shorter, first, because of smaller displacement, and second, because of higher angular velocities.

The time course of joint angles was not monotonic and had small oscillations at the final stage of the movement. The effect of perturbations on muscle torques was significant only at this stage. Therefore, we analyzed viscoelastic properties of the neuromuscular system only at the final stage. An epoch of analysis was 300 ms long. The beginning was set at the point of crossing between the two orthogonal average trajectories (Fig. 1), i.e., at around 150–300 ms from movement onset across the subjects. Borders of the epoch of analysis for the subject#1 are marked by the vertical lines on the plots in Fig. 3.

The standard deviation of muscle torques from their mean values across the epoch of analysis over all subjects ranged between 0.7 and 1.2 Nm for transverse unperturbed movements, and between 1.0 and 2.6 Nm for forward unperturbed movements. The mean square difference between muscle torques during perturbed and unperturbed movements was 3.7–6.0 Nm for transverse movements and 4.2–5.6 Nm for forward movements. Thus, the effect of perturbations significantly exceeded variability of natural unperturbed movements.

4.5 Viscoelastic parameters

The viscoelastic parameters of the arm were obtained from the linear regression model (2) for each subject and each movement direction over all trials including those without perturbation. The regression equation was solved with eight parameters: S_{11}, $S_{12} = S_{21}$, S_{22}, V_{11}, $V_{12} = V_{21}$, V_{22}, T_1^0 and T_2^0 for each time moment.

Figure 4 shows the dependence of the mean square error of the regression model on the time delay τ for subject#1 over the epoch of analysis, the best approximation being achieved for this subject at a delay of around 60 ms (between 40 to 60 ms for all subjects). In all subsequent calculations the value of 50 ms was used as an optimal estimate of the time delay in the regression model (2) for all subjects. For this time delay the coefficient of determination R^2 was greater than 0.8 for all time moments inside the epoch of analysis in all subjects.

At the end of the movement, when the arm stopped, the vector of muscle torques $\mathbf{T}$ should be zero, and therefore according to our model, $\mathbf{T}' = \mathbf{T}^0 - \mathbf{S}\theta^{\text{fin}}$ should be zero, where θ^{fin} is the final joint angles. It is interesting to reveal at which moment of the movement $\mathbf{T}'$ became close to zero.

The time courses of the eight regression parameters for subject#1 are shown in Fig. 5. Note that instead of the components of intercept $\mathbf{T}^0$, the components of the vector $\mathbf{T}' = \mathbf{T}^0 - \mathbf{S}\theta^{\text{fin}}$ are shown. They appeared to be small in comparison with the components of the vector of muscle torques $\mathbf{T}$ at the whole epoch of analysis. The stiffness and viscosity coefficients did not vary monotonically in time. As in Gomi and Kawato (1997), the stiffness coefficients increased at the final stage of the movement and decreased when movement ceased. The change of coefficients of stiffness and viscosity in time was statistically significant. However, we were mainly

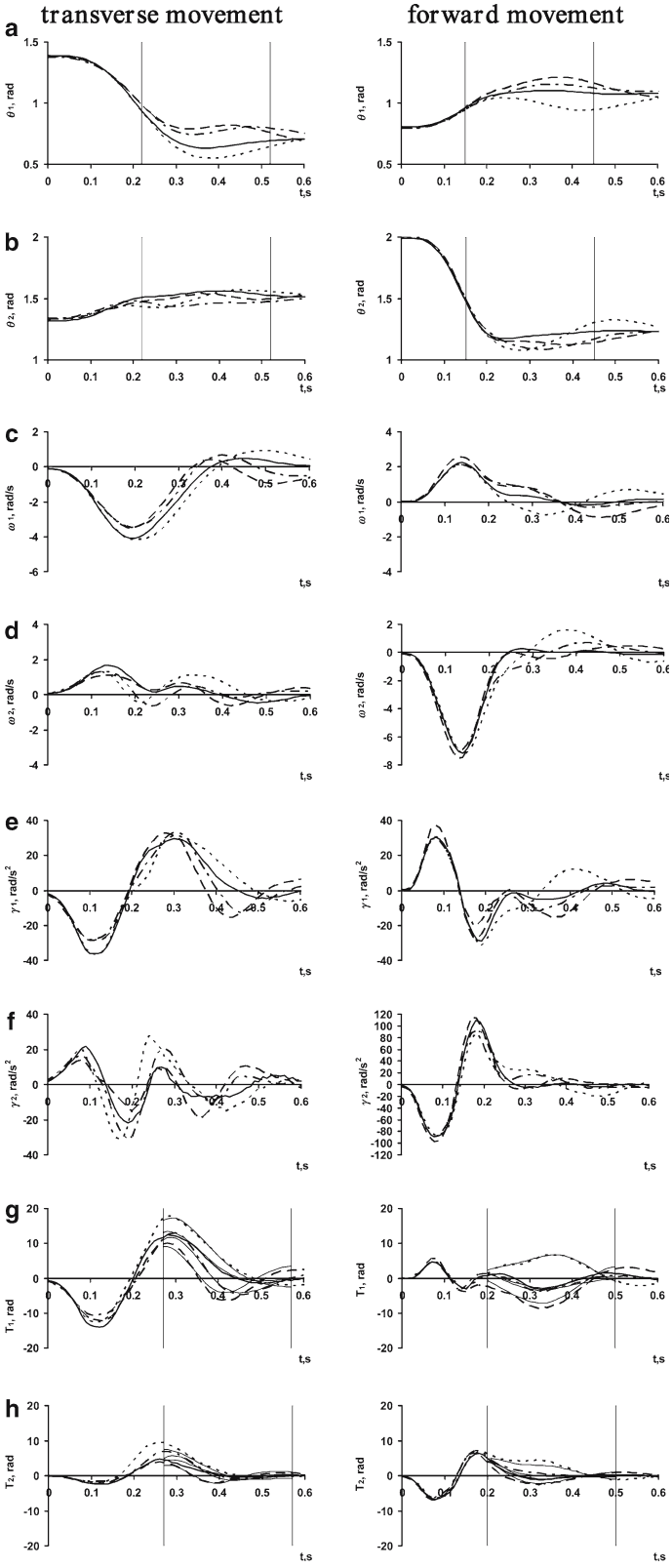

Fig. 3 Time courses of shoulder (**a**) and elbow (**b**) angles, angular velocities (**c** and **d**), angular accelerations (**e** and **f**), muscle joint torques (G and H) for subject#1 averaged over all unperturbed movements (*thick solid lines*), perturbed to the left (*dashed lines*), to the right (*dotted lines*), and forward (*dashed-dotted lines*). The borders of the epoch of analysis are shown by *vertical bars*. *Thin solid lines* in (**g**) and (**h**) are predictions of the regression model (3) with the time delay $\tau = 50$ ms

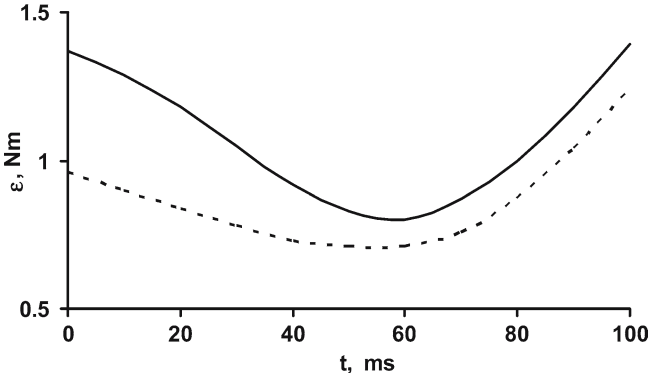

Fig. 4 Dependence of the error ϵ of the regression model (2) on the time delay τ for subject#1. *Solid* and *dashed lines* represent transverse and forward reaching directions, respectively

interested in the dependence of these coefficients on movement direction. We therefore neglected their time dependence and assumed the parameters of the model to be constant during the epoch of analysis. Additionally, we assumed vector $\mathbf{T}' = \mathbf{T}^0 - \mathbf{S}\Theta^{\text{fin}}$ to be zero. In fact, we replaced the regression equation (2) applied to each time moment by the model:

$$\mathbf{T}(t) = -\mathbf{S}[\Theta(t-\tau) - \Theta^{\text{fin}}] - \mathbf{V}\dot{\Theta}(t-\tau), \tag{3}$$

applied to the whole epoch of analysis, where the matrices **S** and **V** are constant. The accuracy of the regression model (3) in approximation of muscle torques, shown in Figs. 3 and 6, demonstrates that the accuracy of the model (3) is close to that of the model (2). In general, over all subjects the error of the model (3) is only about 10% larger than the model (2). Thus, the model (3) with only six regression parameters provides almost the same accuracy as model (2) with 240 parameters (30 time moments by 8 parameters for each time moment).

The coefficients of the matrices of stiffness and viscosity obtained by the regression model (3) are compared in Fig. 5 with those obtained by full regression model (2) for subject#1. Although the difference between coefficients obtained by (3) and those obtained by (2) is statistically significant, in average they are close. Therefore, we used namely these constant coefficients of matrices **S** and **V** obtained by (3) in order to characterize the average viscoelastic properties of a neuromuscular system at the final stage of the movement. Table 2 presents these viscoelastic parameters for all subjects. All coefficients of stiffness and viscosity during forward movements differ significantly from those during transversal movements for all subjects (t-test, $p < 0.05$).

5 Discussion

The stiffness coefficients we obtained for reaching movements in both directions were comparable with those previously obtained by Gomi and Kawato (1997) and Mah (2001). The elbow stiffness ranged over 5–12 Nm/rad, while Gomi and Kawato (1997) reported 5–21 Nm/rad and Mah (2001) reported 2.7–10 Nm/rad. For shoulder stiffness, we obtained 10–31 Nm/rad, while Gomi and Kawato (1997) reported 10–35 Nm/rad and Mah (2001) reported 12–27 Nm/rad. As an overall measure of stiffness, the root mean square (RMS) = $\sqrt{\nu_1^2 + \nu_2^2}$ of eigenvalues ν_1 and ν_2 of the stiffness matrix can be used. In our experiments RMS ranged over 15–37 Nm/rad, while Mah (2001) reported a median value of 30 Nm/rad. However, the obtained values of stiffness coefficients were smaller than values 35–70 Nm/rad for the shoulder and 20–45 Nm/rad for the elbow as described by Franklin et al. (2003).

On the other hand, our values of viscosity coefficients were about twice larger than those of Mah (2001) and an order of magnitude larger than the values obtained during posture maintenance (Tsuji et al. 1995). The coefficients of elbow and shoulder viscosity ranged over 1–3 Nms/rad and 2–6 Nms/rad in our experiments, compared to 0.14–0.78 Nms/rad and 1.2–2.5 Nms/rad, respectively, in the experiments of Mah (2001). Consequently, in the Mah experiments, the contribution of viscous forces to overall muscle torques amounted to only 12%. As shown in Fig. 6, in our experiments the contribution of viscous forces is a dominant component.

The difference in the evaluation of the viscosity coefficients may be explained by the difference in the spring-like linear models that approximate the joint muscle torques as a function of joint angles and angular velocities. We used a spring-like model with a time delay $\tau = 50$ ms, while Mah (2001) and Tsuji et al. (1995) used a model without time delay. In order to explain the underestimation of the viscosity coefficients when the time delay is ignored, let us consider the Taylor expansion of Eq. (2):

$$\begin{aligned}\mathbf{T}(t) &\simeq \mathbf{T}^0 - \mathbf{S}(\Theta(t) - \dot{\Theta}(t)\tau) - \mathbf{V}(\dot{\Theta}(t) - \ddot{\Theta}(t)\tau) \\ &\simeq \mathbf{T}^0 - \mathbf{S}\Theta(t) - (\mathbf{V} - \mathbf{S}\tau)\dot{\Theta}(t)\end{aligned}$$

Thus, viscosity is reduced by $\mathbf{S}\tau$ if time delay is ignored.

Generally muscle damping arises from muscle mechanics themselves (Hill's law) and stretch reflex feedback. The first mechanism has not a time delay whereas the second has the delay of 30–60 ms (Koshland and Hasan 2000). The viscosity coefficients obtained reflect both of these physiological mechanisms. Since our feedback model is optimal under the time delay of 50 ms, it reflects mainly the contribution of the stretch reflex loop. The dominance of stretch reflex loop can be explained particularly by the asymmetry of these mechanisms. The mechanical muscle damping is larger during shortening than during lengthening. In contrast, the stretch reflex damping is larger during lengthening than during shortening. At the second half of the movement which was analyzed, the muscles that stop the movement are mainly activated and just these muscles are lengthened. Hasan (1983) have shown that dynamic coefficient of stretch reflex feedback amounts to about 0.1 of its static coefficient. This defines the ratio of viscosity coefficient to stiffness coefficient in stretch reflex loop if time delay is taken into account. The magnitudes of viscosity coefficients obtained in our study are in this physiological range.

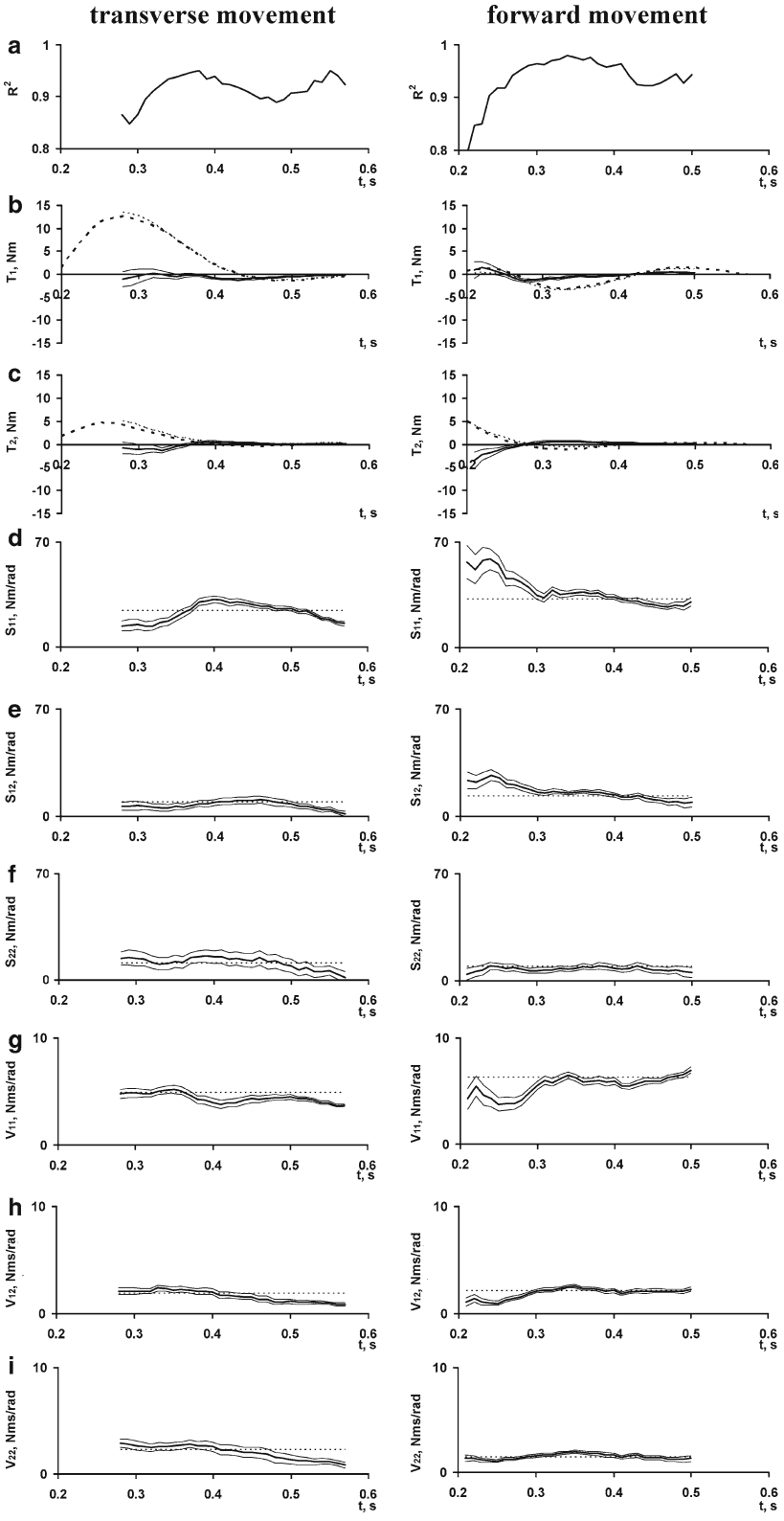

Fig. 5 Time course of the coefficient of determination R^2 (**a**), components of the model intercept $\mathbf{T}^0 - \mathbf{S}\boldsymbol{\theta}^{\text{fin}}$ for shoulder (**b**) and elbow (**c**) joints, coefficients of stiffness S_{11} (**d**), $S_{12} = S_{21}$ (**e**), S_{22} (**f**), and coefficients of viscosity V_{11} (**g**), $V_{12} = V_{21}$ (**h**), V_{22} (**i**) obtained by the regression model (2) for transverse and forward movements for subject#1 (*thick solid lines*). Only the epoch of analysis is shown. *Thin solid lines* represent standard errors. *Thick dashed lines* in (**b**) and (**c**) are components of the muscle torque $\mathbf{T}(t)$ measured experimentally and averaged over unperturbed movements. *Thin dashed lines* are model predictions. *Horizontal dotted lines* in (**d**–**i**) are average viscoelastic coefficients obtained by the regression model (3)

Table 2 Viscoelastic parameters in the reaching movements

Subject	Transverse				Forward			
	S (Nm/rad)		V (Nms/rad)		S (Nm/rad)		V (Nms/rad)	
1	24.9±2.4	8.4±2.6	5.0±0.2	1.8±0.2	31.3±2.2	12.9±1.5	6.3±0.3	2.1±0.1
	8.4±2.6	9.6±6.3	1.8±0.2	2.1±0.5	12.9±1.5	9.7±1.9	2.1±0.1	1.4±0.1
2	13.3±1.4	5.0±1.2	2.2±0.1	1.1±0.1	26.0±2.0	12.8±1.1	4.7±0.3	1.8±0.1
	5.0±1.2	8.3±2.2	1.1±0.1	1.8±0.3	12.8±1.1	7.1±1.1	1.8±0.1	1.1±0.1
3	10.8±3.1	5.4±2.8	2.5±0.2	1.2±0.2	19.7±1.8	8.8±1.0	5.1±0.3	2.0±0.1
	5.4±2.8	8.6±5.6	1.2±0.2	1.8±0.4	8.8±1.0	5.1±0.9	2.0±0.1	1.1±0.1
4	16.1±1.5	7.9±1.4	3.4±0.2	2.0±0.2	24.2±3.7	12.4±2.3	3.8±0.6	1.6±0.2
	7.9±1.4	11.7±3.1	2.0±0.2	2.7±0.4	12.4±2.3	7.2±2.2	1.6±0.2	1.3±0.2

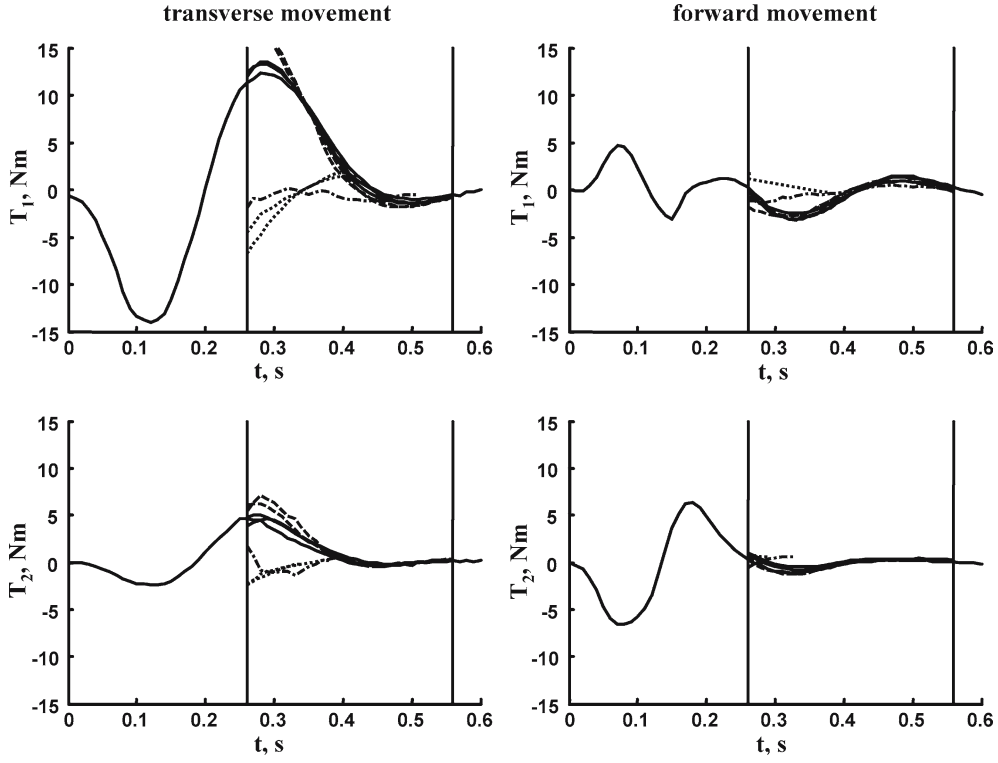

Fig. 6 Time course of components of the muscle torque $\mathbf{T}(t)$ for transverse and forward unperturbed reaching movements for subject#1. *Solid lines*: averaged experimental data and predictions of the regression models (2) and (3). *Dashed and dotted lines*: viscous and elastic components of the model torque. *Dashed-dotted lines*: the component $\mathbf{T}' = \mathbf{T}^0 - \mathbf{S}\Theta^{\text{fin}}$ of torque in the model (2). The time delay was set to $\tau = 50$ ms

Due to the time delay τ in our models (2) and (3), it is impossible to compare quantitatively the matrices of stiffness and viscosity in Cartesian space with numerous results of other researchers. The force generated by the arm $\mathbf{F}_{in} = \left(\mathbf{J}^T\right)^{-1}\mathbf{T}$ in Cartesian coordinates depends on the hand position both at time t and at time $t - \tau$. Therefore, transformation of stiffness and viscosity matrices from joint angle space into Cartesian space can be performed only approximately when dependence of Jacobian on the hand position is ignored. In this approximation, the matrices of stiffness $\mathbf{S}_C$ and viscosity $\mathbf{V}_C$ in Cartesian space are determined by the equations:

$$\mathbf{S}_c = \mathbf{J}^{-1^T}\mathbf{S}\mathbf{J}^{-1}, \quad \mathbf{V}_C = \mathbf{J}^{-1^T}\mathbf{V}\mathbf{J}^{-1}. \tag{4}$$

These matrices can be graphically represented by ellipses (e.g. Mussa-Ivaldi et al. 1985). In our model, the matrices $\mathbf{S}$, $\mathbf{V}$ are symmetric and positive definite, and thus $\mathbf{S}_C$ and $\mathbf{V}_C$ are also symmetric and positive definite. Their eigenvectors are directed along the axes of the ellipses, and their eigenvalues are positive and equal to the lengths of these axes. Displacement of WP in a direction of the ellipse axis leads to a restoring force directed along this axis. The force will be maximal for the major axis and minimal for the minor axis.

Figure 7 shows the ellipses of the stiffness matrices $\mathbf{S}_C$ in Cartesian space. The Jacobian $\mathbf{J}$ in Eq. 4 corresponds to the point of crossing of the orthogonal trajectories (Fig. 1). Thus the difference between the matrices $\mathbf{S}_C$ in two orthogonal movements is explained only by the difference in matrices $\mathbf{S}$.

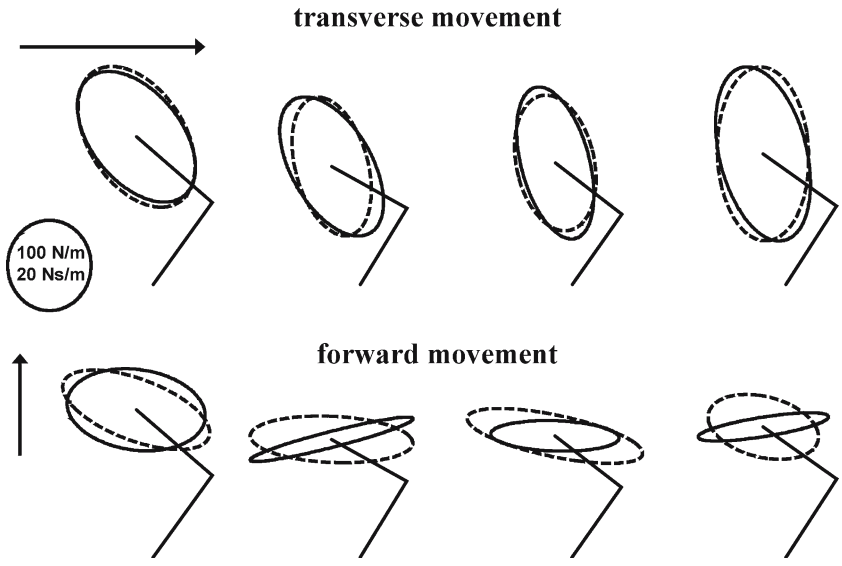

Fig. 7 Ellipses of the stiffness matrix $\mathbf{S}_C$ (*solid lines*) and the viscosity matrix $\mathbf{V}_C$ (*dashed lines*) for both directions of reaching movements in Cartesian hand coordinates

It is known that the major axes of the stiffness ellipses during posture maintenance are generally directed toward the shoulder joint (e.g. Mussa-Ivaldi et al. 1985; Flash and Mussa-Ivaldi 1990). As shown in Fig. 7, during reaching movements these major axes relate more to the direction of movement and are preferentially aligned orthogonally to the movement direction. This is similar to the results of Gomi and Kawato (1997) for transverse direction of movement, although they used longer movement duration ($\sim$1 s). For forward direction of movement, our results are closer to those of Mah (2001) and Franklin et al. (2003), which were obtained for faster movements. The alignment of the stiffness and viscosity ellipses across the movement suppresses unexpected external perturbations preferentially orthogonally to the movement direction. Therefore we can suggest that the functional meaning of this alignment is path preserving.

Another suggestion on the observed dependence of viscoelastic properties on movement direction relates to the equilibrium point (EP) hypothesis (Feldman 1979; Feldman and Levin 1995). In terms of this hypothesis, Eq. 2 can be rewritten in the form:

$$\mathbf{T}(t) = \mathbf{S}(\theta^{eq}(t) - \theta(t-\tau)) - \mathbf{V}\dot{\theta}(t-\tau), \qquad (5)$$

where $\theta^{eq}(t) = \mathbf{S}^{-1}\mathbf{T}^0(t)$. The EP hypothesis suggests that the virtual trajectory of the equilibrium point is simple and close to the actual trajectory of the reaching movement. Then movement planning can be performed in terms of a simple shift of the equilibrium point from its initial to final position, with each position along the planned trajectory being treated by the motor control system as an equilibrium position. The motor control system only needs to compute the control signals required to stabilize the arm in each virtual position. This hypothesis implies that the brain has a built-in internal representation (or internal model) of the executive system that includes body geometry and properties of the neuromuscular apparatus, i.e. a static internal model. Another, quite different hypothesis is that control signals are established by solving the inverse dynamic problem (Kawato et al. 1987), i.e. the brain creates an internal model of the executive system which takes into account not only its static but also its dynamic properties.

According to the EP hypothesis, θ^{eq} reaches the final position θ^{fin} at the first half of the movement and remains to be constant $\theta^{eq} = \theta^{fin}$ until the movement offset (Feldman and Levin 1995). This is consistent with our observations: at the final stage of the movement muscle torques are rather accurately described by the regression model (3), which is equivalent to Eq. 5 where $\theta^{eq} = \theta^{fin}$. Thus at the final stage of the movement our results are in agreement with EP hypothesis.

Katayama and Kawato (1993) argued against the EP hypothesis. They showed by computer simulation that the equilibrium hand trajectory is quite different from the actual trajectory for a range of stiffness equal or below 20 Nm/rad at the shoulder and 15 Nm/rad at the elbow. In our experiments, shoulder stiffness was smaller than 20 Nm/rad for transverse movements in three out of four subjects and in one subject for forward movements, whereas the elbow stiffness was smaller than 15 Nm/rad for all subjects in both movement directions. Thus, one could expect that with these viscoelastic parameters the equilibrium and actual trajectories would be different. We checked this with a computer simulation for transverse reaching movements. We used inertial and viscoelastic parameters obtained for subject#1 and set matrices $\mathbf{S}$ and $\mathbf{V}$ to be constant during the whole movement. The trajectory $\theta^{eq}(t)$ was set to be a straight line in Cartesian coordinates of WP. The equilibrium WP position moved along this trajectory from initial to final position with a constant velocity during 200 ms. The WP trajectory obtained by solving (1) is shown in Fig. 8 by the dashed line.

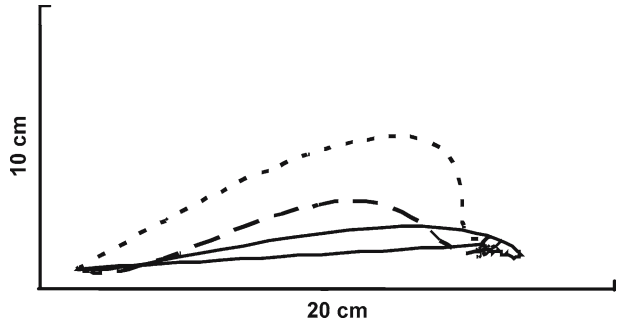

Fig. 8 Transverse trajectories of the working point obtained experimentally and by computer simulations for subject#1. *Thick solid line*: experimental trajectory averaged over all transverse unperturbed movements. *Thin solid line*: equilibrium point trajectory. *Dashed* and *dotted lines*: trajectories computed with viscoelastic parameters obtained for transverse and forward movements, respectively

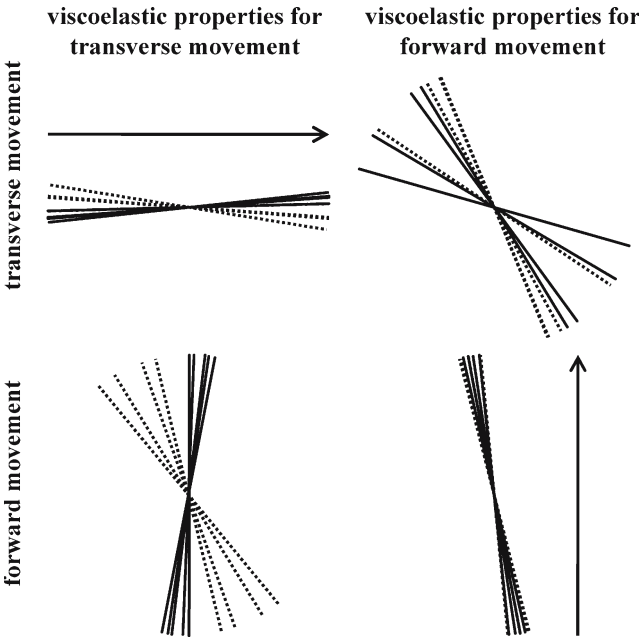

Fig. 9 Directions of vectors $\mathbf{d}_1 = \mathbf{S}_C^{-1}\mathbf{I}_C\mathbf{d}$ (*dotted lines*) and $\mathbf{d}_2 = \mathbf{S}_C^{-1}\mathbf{V}_C\mathbf{d}$ (*thin solid lines*) calculated for both transverse and forward movement directions $\mathbf{d}$(*thick solid lines*) with the use of viscoelastic parameters obtained for both transverse and forward movements

The same calculation for *transverse* movement was made with the viscoelastic parameters obtained for *forward* movement (Fig. 8, dotted line). The WP transverse trajectory calculated with the coefficients obtained in *forward* direction is farther away from the equilibrium trajectory than the WP trajectory calculated with the coefficients obtained in *transverse* direction. Despite the fact that the stiffness coefficients were higher for *forward* direction than those for *transverse* direction (see Table 2, subject#1). Hence the deviation of the actual trajectory from the equilibrium trajectory depends not only on the values of the stiffness coefficients, but also on their distribution, which determines the orientation of the stiffness ellipse.

The question arises of how stiffness and viscosity ellipses must be oriented in order to provide the WP movement $\mathbf{r}(t)$ along the same straight line as the equilibrium trajectory $\mathbf{r}^{\mathrm{eq}}(t)$. Let us consider the motion equation for WP in linear approximation:

$$\mathbf{I}_C\ddot{\mathbf{r}}(t) + \mathbf{V}_C\dot{\mathbf{r}}(t-\tau) + \mathbf{S}_C\mathbf{r}(t-\tau) = \mathbf{S}_C\mathbf{r}^{\mathrm{eq}}(t) \qquad (6)$$

where matrices $\mathbf{I}_C, \mathbf{V}_C$ and $\mathbf{S}_C$ are assumed to be constant. Let the desired movement of WP be $\mathbf{r}(t) = \mathbf{r}(0) + \mathbf{d}\xi(t)$, where $\mathbf{r}(0)$ is WP initial position, $\mathbf{d}$ is a direction of the trajectory and $\xi(t)$ is the desired time course of WP displacement along this direction. According to (6), the equilibrium trajectory which provides this WP movement is

$$\mathbf{r}^{\mathrm{eq}}(t) = \mathbf{r}(0) + \mathbf{d}_1\ddot{\xi}(t) + \mathbf{d}_2\dot{\xi}(t-\tau) + \mathbf{d}\xi(t-\tau)$$

where $\mathbf{d}_1 = \mathbf{S}_C^{-1}\mathbf{I}_C\mathbf{d}$and $\mathbf{d}_2 = \mathbf{S}_C^{-1}\mathbf{V}_C\mathbf{d}$. Since time courses of the variables $\ddot{\xi}(t), \dot{\xi}(t-\tau)$ and $\xi(t-\tau)$ are generally quite different, the trajectory $\mathbf{r}^{\mathrm{eq}}(t)$ is straight only if vectors $\mathbf{d}_1$ and $\mathbf{d}_2$ have the same direction as vector $\mathbf{d}$. This is quite in line with our experimental observation. Figure 9 demonstrates the directions of vectors $\mathbf{d}_1$ and $\mathbf{d}_2$ calculated for both transverse and forward directions $\mathbf{d}$ with the use of viscoelastic parameters obtained for both transverse and forward movements. It is shown that directions of $\mathbf{d}_1$, $\mathbf{d}_2$ and $\mathbf{d}$ are close to each other if viscoelastic parameters measured for the movement in the same direction were used and they were different in the opposite case. Thus, the obtained orientations of stiffness and viscosity ellipses in dependence on movement direction are consistent with EP hypothesis.

In principle, one could suggest that rotation of stiffness and viscosity ellipses according to rotation of the movement direction is explained by "asymmetry" in the experimental design: during transverse movements, the force of perturbation in average was orthogonal to the movement trajectory and during forward movements it was along the trajectory. Then perturbation during transverse movement produces activation of muscles stabilizing the arm in the direction orthogonal to the movement. It is known that the contribution of each muscle to joint stiffness is proportional to its activation (Gomi and Osu 1998). Thus, the observed large stiffness in the direction orthogonal to the transverse movement could result from the activation of corresponding muscles due to perturbation. During forward movements, perturbation along the trajectory was applied at the second phase of movement when muscle forces stopping the arm were directed opposite to the perturbation. Thus muscles stopping the arm were additionally activated to resist perturbation. This could increase stiffness in the direction of movement. However, in our experiments we observed that the stiffness is less in the direction along the trajectory. Therefore, the observed orientations of stiffness and viscosity ellipses for transverse and forward movements cannot be explained by the mentioned asymmetry in the experimental design.

"Asymmetry" in the experimental design could result also in adaptation of the movement control to the general direction of perturbations. In order to reveal this effect the first movements (dashed lines) of series in a given direction were compared with the last movements (solid lines) in Fig. 10. Since

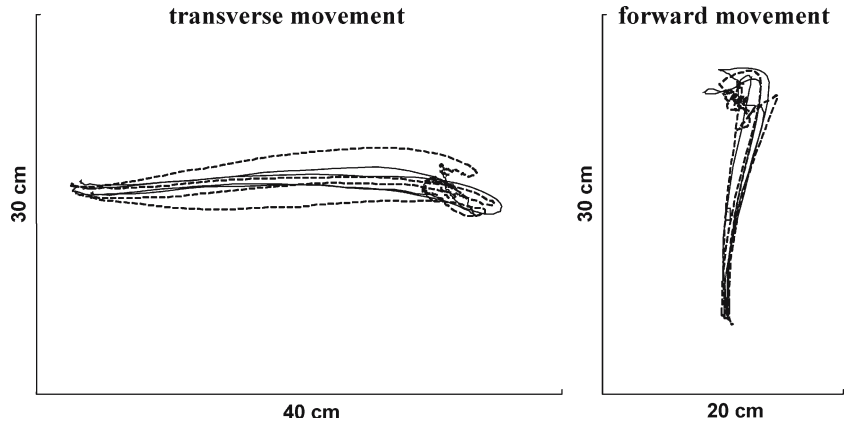

Fig. 10 First (*dashed lines*) and last (*solid lines*) trajectories of unperturbed movements in the series with perturbations for subject#1

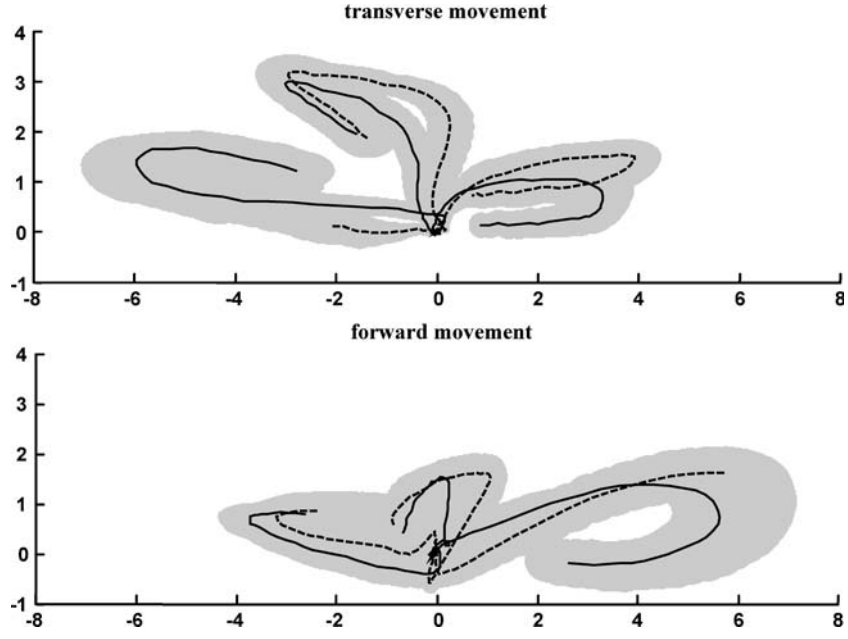

Fig. 11 Deviations of the first (*dashed lines*) and the last (*solid lines*) trajectories of perturbed movements from averaged unperturbed trajectories for each direction of movement and each direction of perturbation averaged over the series and the subjects. The standard errors are shown by the *gray area*

the perturbing system was in front of the subjects (Fig. 1) one could expect anticipatory increase of muscle forces to prevent forward perturbation. As a result the last unperturbed trajectories in the series of transverse movements should be slightly curved in backward. However, this effect was not observed. The first and last trajectories were uniformly mixed without systematic dependence of their curvature upon the number of movement in series. For all the subjects the difference between joint angles at any time moment in the first and last movements in series was not significant (t-test, $p > 0.05$).

The adaptation to perturbations could be also manifested in the change of viscoelastic parameters. It was shown (Burdet et al. 2001; Franklin et al. 2003) that these parameters can adapt without the change of unperturbed trajectory. In order to check this possibility, perturbed trajectories of the first movements (dashed lines) of series in a given direction were compared with perturbed trajectories of the last movements (solid lines). The deviation of perturbed trajectories from averaged unperturbed trajectories are presented in Fig. 11. The standard errors are shown by the gray area. During right and forward perturbations in transverse movements and during left perturbations in forward movements, hand deflections in forward direction in the first movements are larger than those in the last movements. Thus the effect of adaptation of viscoelastic parameters to frontal perturbations was actually observed. However we believe that this effect was not essential. It could influence elongation of the stiffness ellipse in the transverse movement but the orientation of the stiffness ellipse in the forward movement is opposite to this effect.

The adjustment of viscoelastic properties to movement direction could be explained by the peculiarities of the neuromuscular system of the human arm, where movements in different directions are provided by different sets of muscles, and the distribution of muscle activities during reaching movements might be the reason for the dependence of viscoelastic properties on movement direction according to Gomi and Osu (1998). Observations in humans showing that they cannot voluntarily change the orientation of stiffness ellipse, even after training (Perreault et al. 2002), favors such an assumption. However, Franklin et al. (2003) have shown that humans can learn to stabilize movement by selectively adjusting the orientation of stiffness ellipse without modification of joint torques. Moreover, our experimental data demonstrate that along the movement direction stiffness is minimal, whereas muscular activity is obviously maximal. Therefore, it is more plausible that the observed orientation of stiffness and viscosity ellipses, i.e. orthogonal to the movement direction, can be learned by motor experience. This orientation is in line with the observation that accuracy of reaching movement is higher orthogonal to the movement than that along the movement (Gordon et al. 1994). The learning procedure could be similar to the learning of optimal feedback movement control under noise conditions as suggested by Todorov and Jordan (2002).

Acknowledgements This work was supported by the RFBR projects 04-04-48989 and 04-01-00215, and by the French CNRS project Robea 2001. We thank Christine Maier for revising our English.

References

Bennett DJ, Hollerbach JM, Xu Y, Hunter IW (1992) Time varying stiffness of human elbow joint during cyclic voluntary movement. Exp Brain Res 88:433–422

Bennett DJ (1994) Stretch responses in the human elbow joint during a voluntary movement. J Physiol (Lond) 474:339–351

Biryukova EV, Roschin VY, Frolov AA, Ioffe ME, Massion J, Dufosse M (1999) Forearm postural control during unloading: anticipatory changes in elbow stiffness Exp Brain Res 124:107–117

Biryukova EV, Roby-Brami A, Frolov AA, Mokhtari M (2000) Kinematics of human arm reconstructed from spatial tracking system recordings. J Biomech 33:985–995

Burdet E, Osu R, Franklin DW, Milner TE, Kawato M (2001) The central nervous system stabilizes unstable dynamics by learning optimal impedance. Nature 414:446–449

Cesari P, Shiratori T, Olivato P, Duarte M (2001) Analysis of kinematically redundant reaching movements using the equilibrium-point hypothesis. Biol Cybern 84:217–226

Domen K, Latash ML, Zatsiorsky VM (1999) Reconstruction of equilibrium trajectories during whole-body movements. Biol Cybern 80:195–204

Feldman AG (1979) Central and reflex mechanisms of motor control (in Russian). Nauka, Moscow

Feldman AG, Levin MF (1995) The origin and use of positional frames of reference in motor control. Behav Brain Sci 18:723–806

Flanagan AG, Ostry DJ, Feldman AG (1993) Control of trajectory modification in target-directed reaching. J Mot Behav 25:140–152

Flash T (1987) The control of hand equilibrium trajectories in multi-joint arm movements. Biol Cybern 57:257–274

Flash T, Mussa-Ivaldi FA (1990) Human arm stiffness characteristics during the maintenance of posture. Exp Brain Res 82: 315–326

Franklin DW, Burdet E, Osu R, Kawato M, Milner TE (2003) Functional significance of stiffness in adaptation of multijoint arm movements to stable and unstable dynamics. Exp Brain Res 151(2):145–157

Frolov AA, Dufossé M, Řízek S, Kaladjian A (2000) On the possibility of linear modelling the human arm neuromuscular apparatus. Biol Cybern 82:499–515

Gomi H, Kawato M (1997) Human arm stiffness and equilibrium-point trajectory during multi-joint movement. Biol Cybern 76(3):163–171

Gomi H, Osu R (1998) Task-dependent viscoelasticity of human multijoint arm and its spatial characteristics for interaction with environments. J Neurosci 18(21):8965–8978

Gordon J, Ghilardi MF, Ghez C (1994) Accuracy of planar reaching movements. I. Independence of direction and extent variability. Exp Brain Res 99(1):97–111

Gribble PL, Ostry DJ, Sanguineti V, Laboissiére R (1998) Are complex control signals required for human arm movement? J Neurophysiol 79:1409–1424

Hasan Z (1983) A model of spindle afferent response to muscle stretch. J Neurophysiol 49(4):989–1006

Hogan N (1985) The mechanics of multi-joint posture and movement control. Biol Cybern 52:315–331

Katayama M, Kawato M (1993) Virtual trajectory and stiffness ellipse during multi-joint arm movement predicted by neural inverse models. Biol Cybern 69:353–362

Kawato M, Furukawa K, Suzuki R (1987) A hierarchical neural-network model for control and learning of voluntary movement. Biol Cybern 57:169–185

Koshland GF, Hasan Z (2000) Electromyographic responses to a mechanical perturbation applied during impending arm movements in different directions: one-joint and two-joint conditions. Exp Brain Res 132(4):485–499

Lacquaniti F, Carrozo M, Borghese NA (1993) Time-varying mechanical behavior of multijointed arm in man. J Neurophysiol 69:1443–1463

Mah CD (2001) Spatial and temporal modulation of joint stiffness during multijoint movement. Exp Brain Res 136:492–506

Mussa-Ivaldi FA, Hogan N, Bizzi E (1985) Neural, mechanical, and geometric factors subserving arm posture in humans. J Neurosci 5:2732–2743

Perreault EJ, Kirsch RF, Crago PE (2002) Voluntary control of static endpoint stiffness. J Neurophysiol 87:2808–2816

Prokopenko RA, Frolov AA, Biryukova EV, Roby-Brami A (2001) Assessment of the accuracy of a human arm model with seven degrees of freedom. J Biomech 34:177–185

Shadmehr R, Arbib MA (1992) A mathematical analysis of the force-stiffness characteristics of muscles in control of a single joint system. Biol Cybern 66:463–477

Shadmehr R (1993) Control of equilibrium position and stiffness through postural modules. J Mot Behav 25:228–241

Stein RB, Kearney RE (1995) Nonlinear behavior of muscle reflexes at the human ankle joint. J Neurophysiol 73: 65–72

Todorov E, Jordan MI (2002) Optimal feedback control as a theory of motor coordination. Nat Neurosci. 5(11):1226–1235

Tsuji T, Morasso P, Goto K, Ito K (1995) Human hand impedance characteristics during maintained posture in multi-joint arm movements. Biol Cybern 72:475–485

Winters JM, Stark L (1987) Muscle models: what is gained and what is lost by varying model complexity. Biol Cybern 55:403–420